

A Spectroscopic Variant of the Light-Harvesting 1 Core Complex from the Thermophilic Purple Sulfur Bacterium *Thermochromatium tepidum*

Yukihiro Kimura,^{*,†,‡} Yuta Inada,[‡] Long-Jiang Yu,[§] Zheng-Yu Wang,[§] and Takashi Ohno[‡]

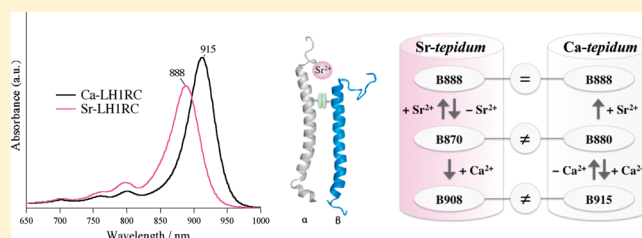
[†]Organization of Advanced Science and Technology, Kobe University, Nada, Kobe 657-8501, Japan

[‡]Department of Agrobioscience, Graduate School of Agriculture, Kobe University, Nada, Kobe 657-8501, Japan

[§]Faculty of Science, Ibaraki University, Bunkyo, Mito 310-8512, Japan

S Supporting Information

ABSTRACT: *Thermochromatium tepidum* is a purple sulfur photosynthetic bacterium, and its light-harvesting 1 reaction center (LH1RC) complexes exhibit an unusual LH1 Q_y absorption at 915 nm (B915) and possess enhanced thermal stability. These unique properties are closely related to an inorganic cofactor, Ca²⁺. Here, we report a spectroscopic variant of LH1RC complexes from *Tch. tepidum* cells in which Ca²⁺ was biosynthetically replaced with Sr²⁺. The photosynthetic growth of wild-type cells cannot be maintained without Ca²⁺ and is heavily inhibited when the Ca²⁺ is replaced with other metal cations. Interestingly, only Sr²⁺ supported photosynthetic growth instead of Ca²⁺ with slightly reduced rates. The resulting Sr-*tepidum* cells exhibited characteristic absorption spectra in the LH1 Q_y region with different LH1RC:LH2 ratios depending on the growth conditions. LH1RC complexes purified from the Sr-*tepidum* cells exhibited a Q_y maximum at 888 nm (B888) that was blue-shifted after removal of Sr²⁺ to ~870 nm (B870). Reconstitution of Sr²⁺ and Ca²⁺ into B870 resulted in red shifts of the Q_y peak to 888 and 908 nm, respectively. The thermal stability of B888 was slightly lower than that of B915 as revealed by differential scanning calorimetry analysis. Effects of other divalent metal cations on the Q_y peak position and thermal stability of B888 were similar but not identical to those of B915. This study provides the first evidence of a purple bacterium in which LH1RC complexes alter spectroscopic and thermodynamic properties in vivo by utilizing exogenous metal cations and improve the ability to adapt to the environmental changes.



Photosynthetic purple bacteria convert light energy into chemical energy through a light-driven redox cycle. This process is initiated by a charge separation of a reaction center (RC) due to the absorption of light energy collected by two types of antenna pigment proteins called light-harvesting complexes, LH1 and LH2.¹ The RC is surrounded by a cylindrical LH1 to form a core complex (LH1RC), and LH2 complexes are located nonstoichiometrically in the periphery of this LH1RC. High-resolution three-dimensional X-ray crystallographic structures are available for RC^{2–4} and LH2 complexes.^{5,6} In contrast, the X-ray structure of the RC associated with the LH1 has been limited to *Rhodospseudomonas palustris* at only moderate resolution.⁷ One RC was stoichiometrically surrounded by one LH1 ring composed of 15 $\alpha\beta$ -subunits with a gap where an unknown protein W was located. This structure was refined on the basis of single-molecule spectroscopy.⁸ Two-dimensional crystallographic studies indicated a variety of LH1 ring forms depending on the species, although their resolutions were insufficient for ascertaining the details of the structural functional consequences in the LH1RC complex.^{9–13} Atomic information about the LH1RC structure is required to clarify the modes of interaction between LH1 and RC complexes or the structural variety of LH1 rings in terms of size and shape, which are significant for understanding

structural stabilities, quinone transport mechanisms, and excited state dynamics of the LH1RC complex.

Photosynthetic purple bacteria have uniquely developed their light-harvesting system to survive under various environments. It is known that peripheral LH2 antenna complexes can adapt to various light conditions and form natural variants by modulating the ring antenna size. The high-resolution crystallographic structures of LH2 demonstrated the nonameric or octameric assembly of $\alpha\beta$ -subunits,^{5,6} and the former was supported by two-dimensional projection maps for *Rhodobacter sphaeroides* and *Rubrivivax gelatinosus*.^{14–16} However, an atomic force microscopy (AFM) study for the native membranes from *Rhodospirillum rubrum* indicated heterogeneity of the LH2 population: not only a major complex with 9-fold symmetry but also an 8- or 10-fold symmetry.¹⁷ A recent study of *Allochrochromatium vinosum* proposed that at least two types of peripheral LH complexes exist, one a 13-mer and the other smaller but larger than a nonamer.¹⁸ Other factors involved in regulating the spectral properties of LH2

Received: February 23, 2011

Revised: April 2, 2011

Published: April 04, 2011

complexes were changes in the hydrogen bonding interaction within the complex cultivated under limited light conditions and the heterogeneity of the $\alpha\beta$ -polypeptide composition. Under low-light conditions, two kinds of LH2 complexes, B800–820 and B800–850, have been reported. The former is found in *Rhodospseudomonas acidophila*¹⁹ and *Rhodospseudomonas cryptolactisi*.²⁰ An FT-Raman study suggested that the blue shift of Q_y bands was caused by alterations of hydrogen bonding interactions between BChl *a* molecules and adjacent polar amino acid residues.²¹ A recent crystallographic structure of B800–820 from *Rps. acidophila* revealed that significant Q_y band shifts were caused by conformational changes in C3-acetyl groups of the BChl *a* dimers, induced by small differences in the hydrogen bonding pattern.²² Another spectroscopic variant B800–850 complex was found in *Rps. palustris*, characterized by much reduced A_{850}/A_{800} ratios^{23–25} and exact 8-fold symmetry.²⁵ The abnormal Q_y absorption property was explained as a heterogeneous $\alpha\beta$ -polypeptide composition, and the complete absence of an 850 nm band in B800–850 was attributed to the LH2 being comprised of one dominant $\alpha\beta_d$ -peptide pair.²⁴

It has been reported that LH1 ring forms vary considerably among different species.^{7–13,26} However, LH1 complexes from the same species are rather insensitive to culture conditions, in contrast to the peripheral LH2. Although the flexibility and size heterogeneity of the LH1 only complex were suggested by an AFM study on RC-lacking mutants from *Rba. sphaeroides*,²⁷ structural and spectral properties were only slightly dependent on the growth conditions for the LH1 complex associated with the RC. The ring size and shape of the LH1 complex assembled by $\alpha\beta$ -subunits seem to be maintained because of interactions with the RC complex during the photosynthetic growth, except for the case of PufX-deleted mutants from *Rba. sphaeroides*, in which formation of S-shaped dimeric LH1RC complexes was suppressed and additional $\alpha\beta$ -subunits were incorporated into LH1 to form a closed ring.^{28,29} Typically, most purple bacteria containing only BChl *a* exhibit an LH1 Q_y maximum around 870–890 nm despite heterogeneity among the species in terms of ring size and shape, exciton coupling, and specific electrostatic interactions.¹ However, some natural species have been reported to show unusual spectral features. Acidophilic *Acidiphilium rubrum* that contains Zn-BChl *a* instead of Mg-BChl *a* exhibited its LH1 Q_y maximum at 864 nm, blue-shifted by ~15 nm from that of *Rhodospirillum rubrum*.³⁰ In contrast, largely red-shifted LH1 Q_y bands have been reported for mesophilic *Roseospirillum parvum* 930I³¹ and strain 970³² at 909 and 963 nm, respectively. The marked red shifts were attributed to interactions between BChl *a* and specific residues on the LH1 polypeptides and/or enhanced exciton coupling within the ringlike assembly of BChl *a* molecules.^{31,32} An alternative species exhibiting abnormal spectroscopic properties is thermophilic *Thermochromatium tepidum*, originally isolated from Mammoth Hot Spring in Yellowstone National Park.³³ This thermophile is a unique photosynthetic purple bacterium in terms of both the unusual LH1 Q_y band at 915 nm (B915), red-shifted by ~25 nm from that of its mesophilic analogue *Ach. vinosum*, and its thermophilic nature, growing at temperatures of up to 58 °C, which is the highest among those of purple bacteria.^{33,34} Recently, we demonstrated that these characteristic properties were closely related with an inorganic cofactor, Ca^{2+} .^{35,36} Upon depletion of Ca^{2+} , the LH1 Q_y band was blue-shifted to 880 nm (B880) with marked deterioration of thermal stability. The modified properties were almost completely restored by following reconstitution of

Ca^{2+} .³⁵ Biochemical replacement of Ca^{2+} with other metal cations revealed that Sr^{2+} -substituted LH1RC exhibited its Q_y peak at 888 nm and had a thermal stability that was approximately 80% of that of the wild-type or Ca^{2+} -reconstituted LH1RC complexes. These results indicate the possibility that Sr^{2+} ions can be functionally replaced by Ca^{2+} in this thermophilic organism.

In this study, we report for the first time a spectroscopic variant of the LH1RC complex obtained from *Tch. tepidum* by utilizing an exogenous inorganic cofactor, Sr^{2+} . *Sr-tepidum* cells in which Ca^{2+} was biosynthetically replaced with Sr^{2+} grew photosynthetically even at temperatures of 50 °C and exhibited different spectral properties in the Q_y region compared with those of wild-type *Tch. tepidum* (*Ca-tepidum*). The purified Sr^{2+} -substituted LH1RC (*Sr*–LH1RC or B888) complex exhibited its Q_y maximum at 888 nm, 27 nm shorter than that of the wild-type LH1RC (*Ca*–LH1RC or B915) complex. The spectral properties and thermal stability of the *Sr*–LH1RC complex were analyzed by absorption, circular dichroism (CD), magnetic CD (MCD), resonance Raman spectroscopy, differential scanning calorimetry (DSC), and sucrose density gradient centrifugation analyses. On the basis of the findings presented here, the structural and functional roles of inorganic cofactors in this thermophilic organism are discussed.

MATERIALS AND METHODS

Culture Conditions. Wild-type *tepidum* cells were cultivated as described previously.³⁷ *Sr-tepidum* cells were obtained by repeated subculturing at 50 °C in a medium containing 0.34 mM $SrCl_2$, instead of $CaCl_2$, under an incandescent lamp for 7–10 days, and cells after the fifth generation were used for sample preparations. To avoid contamination from metal cations other than Sr^{2+} , the culture medium was prepared with deionized distilled water (Simpli Lab, Horiba). For screening growth conditions, absorption intensities at 860 and 910 nm were monitored for the culture cultivated at 45, 50, or 55 °C at light intensities of 10, 40, and 160 $\mu\text{mol m}^{-2} \text{s}^{-1}$. The BChl *a* concentration was estimated from a standard amount of *Sr-tepidum* cell material by extracting BChl *a* with a 7:2 (v/v) acetone/methanol mixture and using the molar extinction coefficient of BChl *a* ($\epsilon_{770} = 76 \text{ mM}^{-1} \text{ cm}^{-1}$).³⁸

Growth Rates. Photosynthetic growth rates of *Tch. tepidum* cells were observed at 40, 50, or 60 °C in the presence of Sr^{2+} or Ca^{2+} and in the absence of both metal cations. After addition of 100 mL of wild-type cells to 1100 mL of each culture medium, the Q_y band intensities at 850 nm were monitored every 24 h for 7 days.

Preparation of LH1RC Complexes. *Ca*–LH1RC complexes were prepared as described previously.³⁷ For *Sr-tepidum*, harvested cells were disrupted in 20 mM Tris-HCl buffer (pH 8.5) by sonication (Sonopuls HD3200, Bandelin), followed by ultracentrifugation (himac CP100WX, Hitachi) at 195000g for 60 min. The resulting chromatophores were first treated with 0.35% (w/v) lauryldimethylamine *N*-oxide at 25 °C for 60 min and ultracentrifuged to remove a large portion of the LH2 complexes. The pellets were further treated with 1.0% (w/v) octyl β -D-glucoside (OG, Anatrace) at 25 °C for 60 min to extract the LH1RC components. After ultracentrifugation, the supernatant was loaded onto a DEAE anion-exchange column (Toyopearl 650S, TOSOH) equilibrated at 4 °C with 20 mM Tris-HCl buffer (pH 7.5) containing 0.08% (w/v) dodecylphosphocholine (DDPC, Anatrace) or 0.8% (w/v) OG. The *Sr-tepidum* LH1RC

components were eluted with a linear gradient of SrCl_2 from 10 to 25 mM, and fractions with an A_{888}/A_{280} of >1.7 were collected. Purification of Sr–LH1RC complexes was also performed by sucrose density gradient centrifugation with a continuous gradient from 10 to 40% (w/v) in 20 mM Tris-HCl buffer (pH 7.5) containing 0.08% DDPC or 0.7% OG.

Depletion of Sr^{2+} from the Sr–LH1RC was conducted according to the procedure reported previously³⁵ with minor modifications. The purified B888 complex was desalted with a size exclusion column (Sephadex G25 M PD10, GE Healthcare) and incubated at 0 °C for 1 h in the dark in the presence of 2 mM ethylenediaminetetraacetic acid (EDTA). The sample solution was extensively washed with a buffer containing 20 mM Tris-HCl (pH 7.5) and 0.08% DDPC using Amicon Ultra 100K (Millipore) to reduce the residual level of EDTA to <1 nM. The effects of metal cations were examined using metal-substituted LH1RC complexes that were prepared via addition of each metal cation (20 mM) to the Sr^{2+} -depleted B888, followed by overnight incubation at 0 °C.

Spectroscopic Measurements. Absorption spectra were recorded on a Shimadzu UV mini1240 spectrophotometer at room temperature. A baseline fitting macro with a low-order polynomial function (TN020 procedure, Igor Pro version 5.05, WaveMetrics) was used for a baseline correction of absorption spectra from *Tch. tepidum* cells. Resonance Raman spectra were recorded with a HoloProbe532 (Kaiser Optics) equipped with an optical microscope (BX60, Olympus) as described previously.³⁹ The excitation light was provided by the frequency-doubled Nd:YAG laser (Showa Optronics). CD and MCD spectra were recorded on a Jasco J-720w spectropolarimeter as described previously,³⁷ with a 20 nm/min scan speed, a 1.0 nm bandwidth, and a 2 s response time. For MCD measurement, an external magnetic field of 1.5 T was applied.

Differential Scanning Calorimetry (DSC). DSC measurements were taken on a nanoDSC II calorimeter (model 6100, Calorimetry Science Co.) in the temperature range of 25–125 °C at a heating rate of 1.0 °C/min.³⁶ In the previous study, we estimated the concentration of the Ca–LH1RC complex by assuming the complex to be a 16-mer of $\alpha\beta$ -polypeptides and using a concentration of BChl *a* molecules extracted from purified LH1RC complexes with a putative molecular mass of ~ 330 kDa.³⁵ In the study presented here, the concentration of B888 was estimated from the LH1 Q_y absorbance of the Sr–LH1RC complex at 888 nm with respect to that of the Ca–LH1RC complex at 915 nm and adjusted to ~ 3.8 mg/mL using Amicon Ultra 100K in a buffer containing 20 mM Tris-HCl (pH 7.5) and 0.08% DDPC in the presence of 20 mM SrCl_2 . The resulting filtrate was used as the reference buffer for the DSC measurement.

RESULTS

Figure 1 shows the time course of cell growth in *Tch. tepidum* at different temperatures monitored with Q_y band intensities at 850 nm. Photosynthetic growth was observed at both 40 and 50 °C in the presence of Sr^{2+} or Ca^{2+} but not in the absence of both metal cations, demonstrating that these metal cations are indispensable cofactors for the biosynthesis in *Tch. tepidum*. In contrast, photosynthetic growth was almost completely inhibited at 60 °C even in the presence of metal cations. Although the rates of formation of the 850 nm band in the presence of Sr^{2+} were slightly decreased relative to those in the presence of Ca^{2+} at

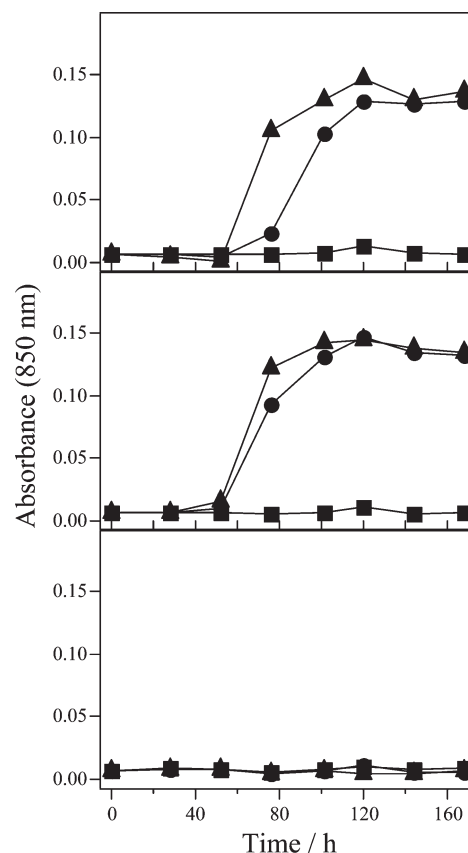


Figure 1. Plots of Q_y band intensity at 850 nm for *Tch. tepidum* cells cultivated at 40 (A), 50 (B), and 60 °C (C) in the presence of Sr^{2+} (●) or Ca^{2+} (▲) or in the absence of both metal cations (■) as a function of cultivation time.

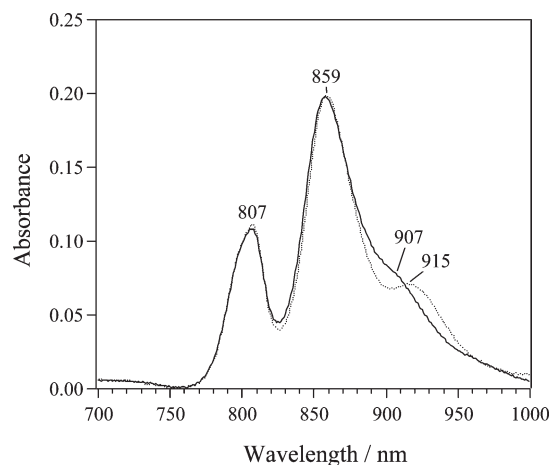


Figure 2. Q_y bands in absorption spectra of Ca-*tepidum* cells (···) and Sr-*tepidum* cells in which Sr^{2+} was biosynthetically substituted for Ca^{2+} (—). These spectra were corrected for light scatter using a baseline fitting program.

both temperatures, the absorbance reached a constant level after cultivation over 120 h.

Figure 2 shows absorption spectra of Sr-*tepidum* (solid line) and Ca-*tepidum* (dotted line) cells in the Q_y band region. Both cells were cultivated anaerobically at 50 °C for 10 days in the

Table 1. Effects of Temperature and Light Intensity on Varying Amounts of BChl *a* and Ratios of LH1RC to LH2 in *Sr-tepidum* Cells

light intensity ($\mu\text{mol m}^{-2} \text{s}^{-1}$)	[BChl <i>a</i>] (mM)			A_{910}/A_{860}		
	40 °C	45 °C	50 °C	40 °C	45 °C	50 °C
10	15	18	19	0.46	0.47	0.47
40	14	15	17	0.39	0.36	0.34
160	13	14	13	0.37	0.34	0.34

presence of each metal cation. The *Ca-tepidum* cells exhibited typical absorption bands at 859 and 807 nm due to the Q_y transitions of BChl *a* molecules for the LH2 and RC complexes and at 915 nm for the LH1 complex. Interestingly, the *Sr-tepidum* cells showed a marked difference in the LH1 Q_y region. The intensity of the 915 nm band decreased, and a new shoulder band appeared around 907 nm; other bands remained unchanged. Because the spectral properties of the extracted LH2 were almost identical between *Ca-tepidum* and *Sr-tepidum* cells (Figure S1 of the Supporting Information), the spectral change induced by the Sr^{2+} substitution is predominantly attributed to the blue shift of the LH1 Q_y absorption. It is notable that the photosynthetic growth was largely suppressed when Ca^{2+} was replaced with other divalent metal cations (Mg^{2+} , Ba^{2+} , and Cd^{2+}). This indicates that observed spectral changes in *Sr-tepidum* cells could not be attributed to nonspecific effects induced by metal cations but originated from specific interactions between Sr^{2+} and the LH1 complex.

During repeated subculturing of the *Sr-tepidum* cells, we found that the absorption properties of the *Sr-tepidum* cells were strongly dependent on the growth temperature and light intensity. To optimize the growth condition, the *Sr-tepidum* cells were cultivated at 40, 45, or 50 °C at light intensities of 10, 40, and 160 $\mu\text{mol m}^{-2} \text{s}^{-1}$. The results are summarized in Table 1, where total concentration of BChl *a* molecules extracted from the cells cultivated under each set of conditions and LH1RC/LH2 populations estimated roughly from A_{910}/A_{860} ratios are presented. The amounts of BChl *a* and LH1RC increased under low-light intensity illumination at each temperature and were maximized under the cultivation at 50 °C with a light intensity of 10 $\mu\text{mol m}^{-2} \text{s}^{-1}$. Although the cells were cultured at temperatures higher than 50 °C (Figure 1C) or lower than 40 °C (data not shown) at different light intensities, the photosynthetic growth was largely suppressed. Therefore, in this study, *Sr-tepidum* cells were cultured at 50 °C at a light intensity of 10–20 $\mu\text{mol m}^{-2} \text{s}^{-1}$, yielding LH1RC-rich *tepidum* cells, which is of great advantage in the purification of the LH1RC complexes.

Figure 3A shows absorption spectra of the purified LH1RC complexes from *Sr-tepidum* (solid line) and *Ca-tepidum* (dotted line) cells. The former (B888) exhibited its LH1 Q_y maximum at 888 nm, blue-shifted by 27 nm from that of B915. In addition, the Soret band at 378 nm and the Q_x band at 592 nm were slightly blue-shifted to 375 and 586 nm, respectively, in the B888 spectrum. In contrast, carotenoid bands at 487, 514, and 550 nm as well as protein bands around 280 nm were affected little by the biosynthetic substitution in the peak position and band intensity. The differences are clearly seen in Figure 3B obtained by subtracting the B915 spectrum from the B888 spectrum. The ratio of the Q_y band intensity at 888 nm relative to the protein band at 280 nm (A_{888}/A_{280}) was ~ 1.7 , lower than

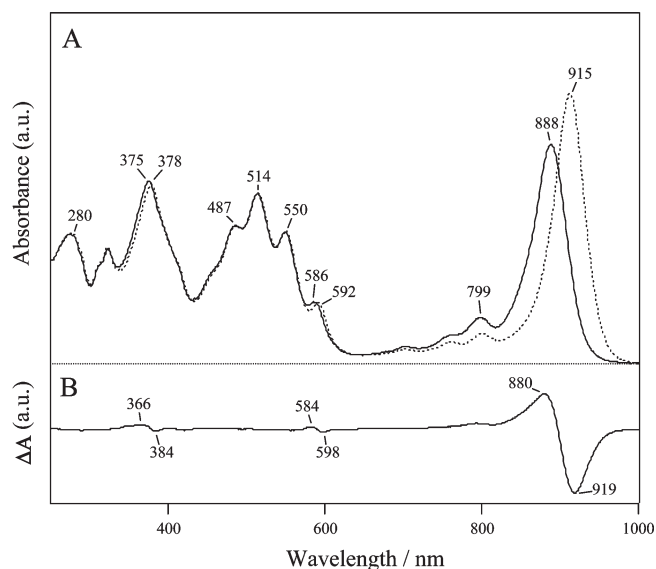


Figure 3. (A) Absorption spectra of the purified Sr–LH1RC complex (B888, —) from *Sr-tepidum* cells and the Ca–LH1RC complex (B915, ···) from *Ca-tepidum* cells. (B) Difference absorption spectrum obtained by subtracting the B915 spectrum from the B888 spectrum after the normalization with respect to the carotenoid band at 514 nm.

that of B915 ($A_{915}/A_{280} > 2.0$). However, this does not indicate a low quality of the sample because the purity of B888 was confirmed by the sodium dodecyl sulfate–polyacrylamide gel electrophoresis profile, where four bands for C, H, M, and L subunits from the RC and two bands for α - and β -polypeptides from the LH1 complex were clearly separated (Figure S2 of the Supporting Information). The purified LH1RC was also obtained by sucrose density gradient ultracentrifugation and showed a Q_y peak around 890 nm in the absence of metal cations (Figure S3 of the Supporting Information). The results strongly support the idea that the Q_y blue shift did not originate from biochemical exchanges of exogenous Sr^{2+} contained in the elution buffer during column chromatography but was the endogenous Sr^{2+} biosynthetically incorporated into the LH1RC during photosynthetic growth.

The purified Sr–LH1RC complex was characterized by CD and MCD spectroscopy. Figure 4A shows the CD spectra of the B888 (solid line) and B915 (dotted line) complexes. The spectral shape of B888 was similar to that of B915 in terms of small and nonconservative signals in the Q_y region, a typical feature for the LH1RC complexes from purple bacteria.⁴⁰ However, negative CD signals in the Q_y regions were clearly different in the B888 and B915 species in response to their Q_y band positions (Figure 3). In addition, CD signals in the Q_x and Soret region also exhibited small but distinctive differences. No other CD signals from accessory BChl *a* molecules in the RC and carotenoid molecules exhibited any significant difference, supporting the fact that the difference between the two species originated from the LH1 BChl *a* molecules. Furthermore, the MCD spectrum of B888 (Figure 4B) exhibited a small positive band at 873 nm and a large negative band at 586 nm corresponding to the Q_y and Q_x transitions, respectively. These bands were slightly blue-shifted versus those of the B915 species (dotted line). The B/D ratio (B , MCD intensity of the Faraday B-term, and D , dipole strength) of the Q_y transition was estimated to be $8.8 \text{ k}\beta/\text{cm}^{-1}$. This value is comparable to those

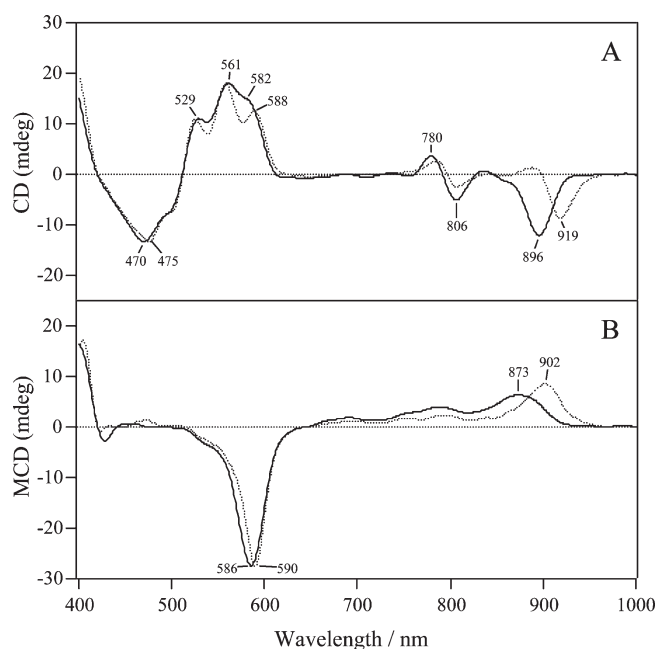


Figure 4. CD (A) and MCD (B) spectra of the LH1RC complexes from *Sr-tepidum* (—) and *Ca-tepidum* (···) cells in the 400–1000 nm range recorded in a buffer containing 20 mM Tris-HCl and 0.08% DDPC (pH 7.5) at room temperature.

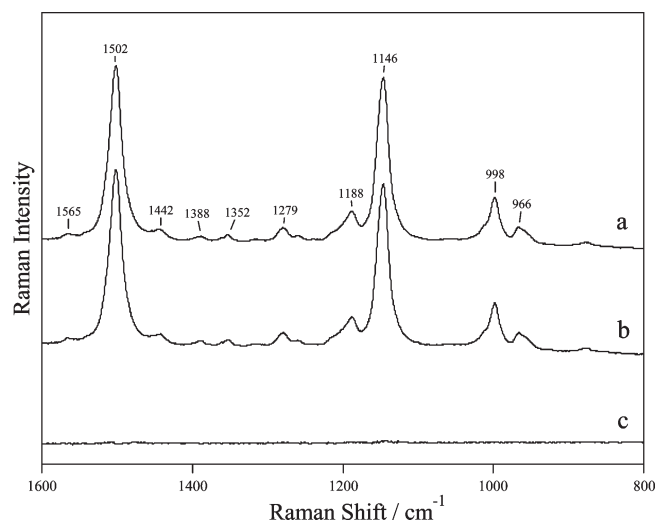


Figure 5. Resonance Raman spectra of the LH1RC complexes from *Sr-tepidum* (a) and *Ca-tepidum* (b) cells obtained by an excitation of the α – β region at 532 nm. The difference between both spectra is also presented (c).

of B915,³⁷ the RC special pair, and LH2 B850 component,⁴¹ suggesting that the 873 nm band originates from the Q_y transition of the BChl *a* dimers. These results confirmed that Sr^{2+} -induced conformational changes in the LH1 BChl *a* dimers are responsible for the blue shift of the B888 species.

Figure 5 shows resonance Raman spectra of B888 (spectrum a) and B915 (spectrum b) complexes obtained by laser excitation at 532 nm, which provides valuable information about the conformation of carotenoid molecules bound to the LH1RC complex. It was reported that most of the carotenoids involved in

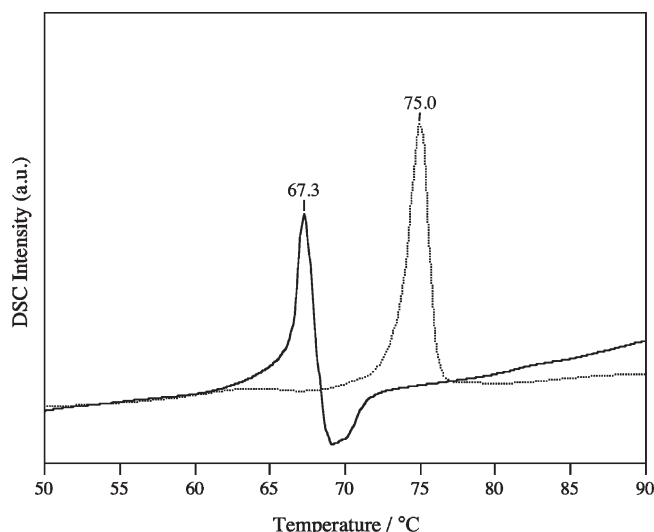


Figure 6. DSC curves of the LH1RC complexes from *Sr-tepidum* (—) and *Ca-tepidum* (···) cells obtained with a heating rate of 1 °C/min in a buffer containing 20 mM Tris-HCl and 0.08% DDPC (pH 7.5). The filtrate from each sample solution was used as a reference. The wild-type curve is from ref 36.

the B915 species were ascribed to spirilloxanthin,³⁷ and thus, intense Raman bands at 1502, 1146, and 966 cm^{-1} were assigned to C=C and C–C stretching modes and the C–H bending mode of all-*trans* spirilloxanthin, respectively.^{42,43} The spectral features of the B888 species were quite similar to those of B915 in their peak position and band intensity, as clearly seen in the difference spectrum (spectrum c). These results support the fact that spirilloxanthin is the major carotenoid also in the B888 species and that the molecular conformation and interaction modes of carotenoid molecules in the LH1RC are almost identical in both B915 and B888.

Next, we examined the thermal stability of the B888 species by DSC analysis. Figure 6 shows the DSC profiles of B888 (solid line) and B915 (dotted line) in the presence of 20 mM SrCl_2 and CaCl_2 , respectively. These DSC bands correspond to the thermal decomposition of the LH1 complexes to the α - and β -polypeptides.³⁶ An intense sharp band of the B888 species appeared with a maximal peak at 67.3 °C, although the thermogram was accompanied by small negative bands around 70 °C, possibly due to the aggregation of proteins. The denaturing peak temperature was lower than that of B915 by 7.7 °C, demonstrating that the Sr–LH1RC complex is thermally unstable compared with the Ca–LH1RC complex. It is particularly worth noting that DSC profiles were largely dependent on the concentration of metal cations. As the concentration of metal cations decreased, the denaturing temperature and band intensity were lowered, along with a broadening of the bandwidth (Figure S4 of the Supporting Information). These results indicate that DSC band shapes also seem to reflect the metal-induced thermal stability of the LH1RC complexes.

To understand the roles of metal cations more closely, effects of various divalent cations on the thermal stability of Sr–LH1RC complexes were examined. Figure 7 shows the effects of Sr^{2+} depletion and the following substitutions of other metal cations on the absorption properties of the B888 species. After the depletion of Sr^{2+} by EDTA (spectrum a), the LH1 Q_y band was largely blue-shifted to 871 nm (B870), which was ~ 10 nm shorter than that of the Ca^{2+} -depleted form of the Ca–LH1RC complex. Similar effects

were confirmed using other metal chelators, suggesting that the blue shift was not caused by specific interactions between EDTA and LH1RC complexes but by the removal of the Sr^{2+} . The Q_y peak returned to its original position (888 nm) upon reconstitution with Sr^{2+} (spectrum d) and Ba^{2+} (spectrum e), and to a lesser extent with Cd^{2+} (spectrum b) and Mg^{2+} (spectrum c). The most significant change was observed after reconstitution of Ca^{2+} , with a red shift to 908 nm (spectrum f). However, a further red shift to 915 nm was not observed in contrast to the results reported for the B915 species.³⁵ These findings implied that B888 and B915 complexes are not compatible with the simple exchange of metal cations but that additional factors are responsible for the differences between the two species.

Next, the thermal stabilities of metal-substituted B888 complexes were examined by monitoring the absorbance at respective Q_y peaks during an incubation at 50 °C (Figure S5 of the Supporting Information). The data after the incubation for 60 min are summarized in Table 2 along with those previously reported for metal-substituted B915 complexes. When no cations were added to B870, the relative intensity of the Q_y band was decreased to less than 9% of the starting absorbance. In the presence of divalent cations (Mg^{2+} , Ca^{2+} , Ba^{2+} , and Cd^{2+}), the B870 complex acquired thermal resistance depending on the cation species in the following order: $\text{Ca}^{2+} > \text{Ba}^{2+} \approx \text{Sr}^{2+} > \text{Mg}^{2+} \gg \text{Cd}^{2+} >$

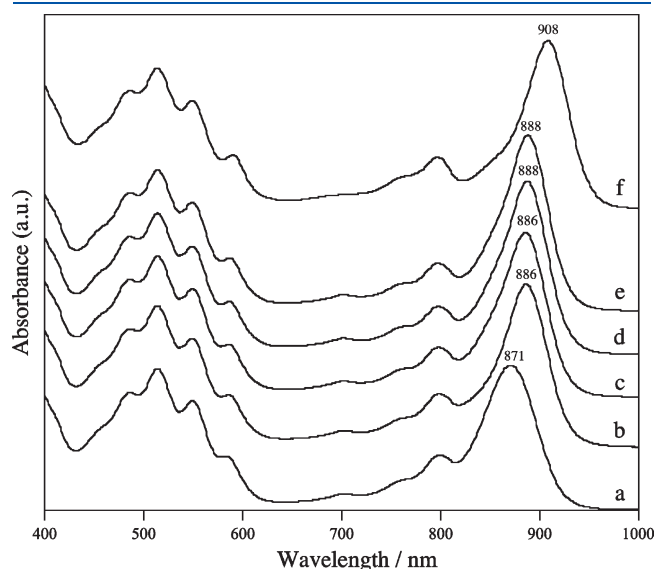


Figure 7. Effects of metal cations on the spectral properties of the LH1RC complexes from *Sr-tepidum* cells. The Sr–LH1RC complex was depleted of Sr^{2+} (a) by EDTA, followed by biochemical replacement with 20 mM Cd^{2+} (b), Mg^{2+} (c), Sr^{2+} (d), Ba^{2+} (e), and Ca^{2+} (f).

none (which was similar with that previously reported for B915³⁶ and closely related with the Q_y maximum of each metal-substituted complex). However, the Q_y peaks of metal-substituted B888 appeared at slightly shorter wavelengths with respect to those of corresponding metal-substituted B915 by 7–10 nm in the presence of Ca^{2+} or no metal cations, and by 2 nm in the presence of other divalent metal cations. In addition, the relative intensity of Q_y bands remaining after incubation at 50 °C decreased by 3–8% compared with those of metal-substituted B915 species other than the Mg^{2+} -bound form. These results imply that metal binding properties and/or the following structural changes are somewhat different between the B888 and B915 species.

DISCUSSION

Spectroscopic Properties of the Sr^{2+} –LH1RC Complex.

This study demonstrates that thermophilic purple sulfur bacterium *Tch. tepidum* can be adapted for anaerobic photosynthetic growth at 50 °C in the presence of Sr^{2+} instead of Ca^{2+} , and the resulting cells exhibited a specific difference in the LH1 Q_y region compared with the wild-type cells (Figure 2). The photosynthetic growth was largely suppressed when Sr^{2+} or Ca^{2+} was removed from the culture medium or replaced with other divalent metal cations, strongly indicating that Sr^{2+} is a single metal cation that can be biofunctionally exchanged with Ca^{2+} in this thermophilic organism. Because the spectroscopic properties of the LH2 complexes were influenced little by the biosynthetic Sr^{2+} substitutions (Figure S1 of the Supporting Information), LH1RC complexes are considered to be responsible for the specific difference in the absorption spectra of the cells. The purified LH1RC complex from the *Sr-tepidum* cells exhibited its Q_y maximum at 888 nm, blue-shifted by 27 nm from that of the Ca–LH1RC complex. The ratio of absorbance for the Q_y band relative to the protein band at 280 nm was lower in the Sr–LH1RC complex (~ 1.7) than in the Ca–LH1RC complex (~ 2.0) because of the decrease in the molar extinction coefficient accompanied by the blue shift of the Q_y peak position.³⁵ CD and MCD analyses revealed that the variation induced by the biosynthetic Sr^{2+} substitution was predominantly attributed to BChl *a* dimers from the LH1 complex. It was reported that small and nonconservative CD signals in the Q_y region reflect strong interaction between BChl *a* and carotenoid molecules.⁴⁰ In addition, blue-shifted carotenoid bands and larger BChl:carotenoid ratios make the CD signal more conservative.⁴⁰ In this study, CD signals in the Q_y region of B888 and B915 were both nonconservative, and the former exhibited a more intense negative band (Figure 4A). However, electronic absorption and resonance Raman bands in the carotenoid region were

Table 2. Effects of Metal Cations on the Spectral and Thermal Properties of LH1RC Complexes

metal cation	ionic radius (Å)	B888		B915 ^a	
		Q_y peak (nm)	Q_y band remaining (%)	Q_y peak (nm)	Q_y band remaining (%)
Ca^{2+}	0.99	908	82.1 (± 3.8)	915	89.3 (± 2.4)
Ba^{2+}	1.35	888	69.6 (± 0.3)	890	73.2 (± 1.7)
Sr^{2+}	1.13	888	66.4 (± 1.0)	890	72.0 (not determined)
Mg^{2+}	0.65	886	57.3 (± 3.1)	888	52.2 (± 5.2)
Cd^{2+}	0.97	886	15.9 (not determined)	888	23.8 (± 4.0)
none	–	871	8.8 (± 5.8)	881	1.8 (± 0)

^aData from ref 36.

identical in both B888 and B915 (Figures 3 and 5). These results suggest that the change in the BChl–carotenoid interactions may not be responsible for the difference in the intensity of the CD signals in both species.

It is notable that replacement of the central Mg^{2+} in BChl *a* molecules with Sr^{2+} during the photosynthetic growth phase is unlikely because BChl *a* molecules extracted from both Sr– and Ca–LH1RC complexes exhibited the identical Q_y peak position at 770 nm in contrast to those of the metal-substituted BChl *a* molecules that were accompanied by minor shifts in their Q_y maxima.^{30,44–46}

Natural Variant of the LH1RC Complex. Generally, peripheral LH2 antenna complexes can adapt to various light conditions to form natural variants.^{14–25} Two types of spectroscopic variants of the LH2 complex have been reported under low-light cultivation. One is the B800–B820 complex from *Rps. acidophila* and *Rps. cryptolactis* that possesses 9-fold symmetry.^{19–22} The blue shift of the Q_y band was attributed to conformational changes in C3-acetyl groups of the BChl *a* molecule, induced by alterations in hydrogen bonding interactions.²¹ The other is the B800–B850 complex from *Rps. palustris* with a much reduced A_{850}/A_{800} ratio and exact 8-fold symmetry.^{23–25} The abnormal Q_y absorption property was attributed to heterogeneity in the composition of the α - and β -apoproteins.²⁴ In contrast, the spectral properties of LH1 complexes from the same species are rather insensitive to the growth conditions, although the flexibility and size heterogeneity of the LH1 complex in the absence of the RC were proposed on the basis of the results of the RC-lacking mutants.²⁷ No evidence has been reported for LH1 complexes associated with the RC showing that the structural and spectral properties were altered depending on the growth conditions. Presumably, specific interactions between the LH1 and RC complexes are responsible for maintaining the ring size and shape of each LH1 complex to ensure that photosynthesis remains functionally normal. It is worth noting that LH1RC complexes from *Rba. sphaeroides* altered the LH1 ring structure from an S-shaped dimeric form to a closed monomeric form because of the deletion of PufX protein.^{28,29} However, this mutant failed to grow photosynthetically, and the spectral features were mostly similar for both the monomeric and dimeric forms despite the modifications in the ring size and/or shape.¹¹ Another interesting species is acidophilic *Ac. rubrum*, which is a unique purple bacterium containing Zn–BChl *a* molecules instead of Mg–BChl *a* molecules, showing its LH1 Q_y maximum at 864 nm.³⁰ Although the LH1 Q_y peak was unusually blue-shifted by ~15 nm compared with that of *Rsp. rubrum*, this bacterium is an aerobic chemoheterotroph and grows under dark and acidic conditions. Accordingly, this study provides the first evidence of a natural variant of the LH1 complex associated with the RC from an anaerobic photosynthetic purple bacterium, induced not by genetic engineering but by utilizing an exogenous inorganic cofactor, Sr^{2+} . It is known that *Tch. tepidum* was isolated from Mammoth Hot Springs in Yellowstone National Park³³ in which mineral calcium carbonate is abundant. To the best of our knowledge, the habitat for this bacterium where Sr^{2+} is present has not been reported. However, this study indicates a possibility that a natural variant of *Tch. tepidum* can grow in the living environment containing abundant Sr^{2+} .

It was demonstrated that Sr^{2+} and Ca^{2+} are indispensable cofactors for photosynthetic growth and the rate in the presence of Sr^{2+} was slightly lower than that in the presence of Ca^{2+} (Figure 1). The difference indicates that these metal cations are

incorporated into the biosynthesis process and Ca^{2+} is more favored than Sr^{2+} for this thermophilic bacterium. Interestingly, Sr^{2+} is the alternative cofactor that can functionally exchange with Ca^{2+} not only in *Tch. tepidum* but also in photosystem II,⁴⁷ which is evolutionarily related to purple bacteria in terms of the heterodimeric reaction center and electron transport system.⁴⁸ In photosystem II, Ca^{2+} ions play essential roles in assembly and photosynthetic oxygen evolution, and Sr^{2+} ions can be functionally replaced with Ca^{2+} to a lesser extent.⁴⁹ Although the structural and functional roles of Ca^{2+} and Sr^{2+} differ in both photosystems, interactions of these cations with their specific protein binding sites may allow the normal functioning of these photosynthetic organisms.

Photosynthetic bacteria are able to adjust their capacity for photon capture in response to the levels of incident light. Aagaard and Sistrom have reported on the variety of the photosynthetic unit (PSU) size in many species.⁵⁰ Generally, the lower the light intensity under which the cells are grown, the greater the increase in the ratio of LH2 complexes to RCs, resulting in the magnification of PSU sizes.⁵¹ Because the LH1RC core complex is relatively insensitive to light intensity, in contrast to the peripheral antenna complexes, cultivation under low-light conditions leads to an increase in the amount of BChl *a* molecules but a decrease in the LH1RC:LH2 ratios, whereas this study revealed that both the LH1RC:LH2 ratio and the BChl *a* concentration increased when the light intensity was reduced, not only in the *Sr-tepidum* cells (Table 1) but also in the *Ca-tepidum* cells (unpublished results). This indicates that effects of light intensity on the biosynthesis of antenna complexes are different from those of typical purple bacteria. A similar tendency was reported for the mesophilic purple sulfur bacterium *Allochrochromatium minutissimum*.⁵² These results suggested that the decrease in light intensity resulted in a decrease in the PSU size but an increase in the LH1RC:LH2 ratio at the optimal physiological temperatures, which is consistent with our results for *Tch. tepidum*. Therefore, the low-light cultivation at physiological temperatures is a useful method for the investigation of purified LH1RC complexes in these species.

Interaction between LH1RC Complexes and Metal Cations. Effects of metal cations on LH1RC complexes from *Sr-tepidum* and *Ca-tepidum* cells and the relationship between both species are illustrated in Figure 8. Depletion of Sr^{2+} from the B888 species resulted in a blue shift of the Q_y band to ~871 nm, and the subsequent reconstitution with Sr^{2+} completely restored its original position. This demonstrates that the interconversion between native and metal-depleted forms in the Sr–LH1RC complex is fully reversible, which is compatible with the results for the Ca–LH1RC complex.³⁵ However, the Q_y peak of B870 was ~10 nm shorter than that of the B880 species obtained from B915 by Ca^{2+} depletion. Furthermore, supplementation of Ca^{2+} for B870 resulted in the formation of the B908 species, of which the LH1 Q_y peak distinctively differed from that of B915. These results indicate that the properties of the metal binding site and/or the following structural and conformational changes are somewhat different between the B888 and B915 species. We cannot completely exclude the possibility that some tightly bound Sr^{2+} ions disturb a complete replacement of Sr^{2+} with Ca^{2+} in the Sr–LH1RC complexes. However, the estimated constant for binding of Sr^{2+} to the B870 species was ~2.5% (unpublished result) with respect to that of binding of Ca^{2+} to the B880 species,³⁵ implying that the 908 nm band is not due to the residual Sr^{2+} tightly bound to the Sr–LH1RC complex. It is interesting to note that Q_y peaks of the Sr–LH1RC complex

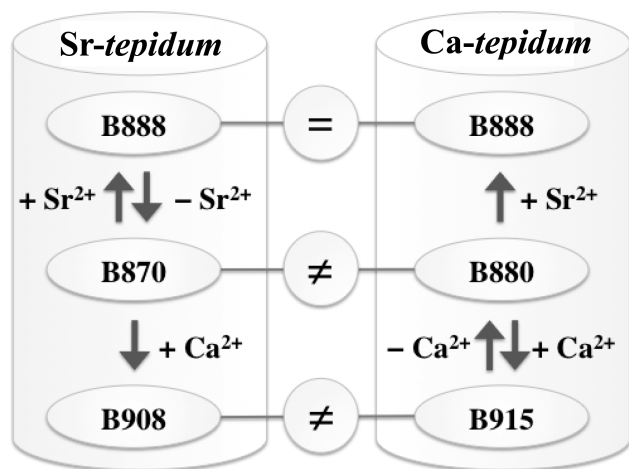


Figure 8. Schematic representation of the relationship between LH1RC complexes from *Sr-tepidum* and *Ca-tepidum* cells and effects of metal cations on both species.

were dependent on the detergent used for the solubilization: peaks at ~ 888 and ~ 905 nm for DDPC and OG, respectively, prepared by both anion-exchange chromatography and sucrose density gradient centrifugation analysis (Figure S3 of the Supporting Information). The inset of Figure S3 shows that the position of the LH1RC component in OG buffer was slightly but distinctively lower than that in DDPC buffer. In addition, the ~ 905 nm band in the presence of OG was blue-shifted to 888 nm after the substitution of the DDPC detergent for OG (data not shown). These results suggest that the aggregation state may be different between these buffer systems. However, such a marked disparity in the effect of the detergent could not be observed in the Ca–LH1RC complex. This may support the idea that there are significant differences between the B888 and B915 species in the modes of interaction of BChl *a* dimers with adjacent amino acids and/or solvent molecules.

This study reveals that spectroscopic properties of carotenoid molecules were little influenced by the biosynthetic Sr^{2+} replacement (Figures 3 and 5) in contrast to BChl *a* molecules, suggesting that the carotenoid binding site in the LH1 $\alpha\beta$ -subunit is not associated with or is separated from the metal binding site. In addition, a study by Stark spectroscopy indicated that the electrostatic environment of the BChl *a* binding site was modified by polar detergent molecules, but this was not the case in the carotenoid binding site.⁵³ Therefore, carotenoid molecules seem to be located in the hydrophobic part of $\alpha\beta$ -polypeptides. This is compatible with the results reported previously that putative Ca^{2+} binding sites are composed of several acidic amino acid residues near the membrane interface of the C-terminal region of the α -polypeptide or the N-terminal region of the β -polypeptide.³⁵ Recently, it was revealed that the former is likely, based on a topological study using *tepidum* chromatophores and metal chelators.⁵⁴ The blue shift of the Q_y bands due to Ca^{2+} depletion by chelators was not induced when the native membranes were completely retained, indicating that the outside of the chromatophore does not include the metal binding site. However, once the membranes were destroyed by detergent treatments, the chelators invaded the inside of the chromatophore where the C-terminus of the LH1 α -polypeptide exists, resulting in a blue shift of the Q_y bands and deterioration of the thermal stability. These results strongly support the idea that the

metal binding site is involved in the C-terminal region of the LH1 $\alpha\beta$ -polypeptide.

Effects of Metal Cations on the Thermal Stability of the LH1RC Complex. In this study, the B888 species exhibited an intense DSC band at 67.3 °C, which was lower by 7.7 °C than that of the B915 species. These DSC bands were ascribed to the decomposition of the core complex to the α - and β -polypeptides,³⁶ demonstrating that the Sr–LH1RC complex is thermally unstable relative to the Ca–LH1RC complex. Judging from the denaturing temperatures of the B888 and B915 species, the thermal stabilities of Sr^{2+} -substituted B888 and Ca^{2+} -substituted B915 in Table 2 evaluated from the thermolysis at 50 °C seem to be low. However, this may be attributed to the difference in the sample concentration; the absorbance at 888 nm was 2.5 and 40 for the absorption and DSC measurements, respectively. In addition, differences in the conditions of both measurements may also be responsible for the difference in thermal stability.

It is interesting that the DSC peaks of B888 and B915 were higher than the temperature used for cultivation (50 °C) and up to 58 °C.³³ In addition, other photosynthetic proteins from *Tch. tepidum* also showed DSC peaks over 70 °C (unpublished results), implying a possibility that this bacterium can grow at temperatures higher than 58 °C. However, photosynthetic growth was completely suppressed with 60 °C cultivation (Figure 1C). Possibly, protein–lipid or –detergent interactions may be closely related to the difference in thermal stability in vitro and in vivo.⁵⁵ In addition, it was reported that ribulose-1,5-bisphosphate carboxylase/oxygenase from *Tch. tepidum* is most catalytically active at 50 °C.^{56,57} Therefore, an optimal temperature for allowing the normal functioning of the photosynthetic apparatus may be around 50 °C, although respective protein complexes are thermally stable up to 70–75 °C.

It is of note that DSC bands of the metal-bound form were sharpened and intense in contrast to those of the metal-depleted form.³⁶ Interestingly, peak temperatures and band shapes of the Ca–LH1RC complex were strongly dependent on the Ca^{2+} concentration (Figure S4 of the Supporting Information). In the native state, the LH1 core complex was firmly retained and drastically decomposed at around 75 °C as revealed by the intense and sharp DSC band. In contrast, the DSC bands appeared at lower temperatures along with broadening and a decrease in intensity after the partial removal of Ca^{2+} by size-exclusion column chromatography or complete removal with chelating agents. A possible explanation is that metal-depleted forms are in an equilibrium involving many different unstable states due to the structural flexibility in the absence of metal cations, which may be responsible for the broadening of the DSC bands. By contrast, metal-bound forms acquired a tightly assembled tertiary structure through the interaction with the metal cations and, therefore, exhibited intense and narrow bands.

The thermal stabilities of the B888 species in which Sr^{2+} was substituted with other divalent metal cations were evaluated by absorption spectroscopy and determined to exist in the following order: $\text{Ca}^{2+} > \text{Ba}^{2+} \approx \text{Sr}^{2+} > \text{Mg}^{2+} \gg \text{Cd}^{2+} > \text{none}$ [in accordance with the results for the B915 species (Table 2)]. However, most metal-substituted forms of B888 showed decreases in both the Q_y peak positions and thermal stability as compared with those from B915. The small but significant differences indicate that the B888 and B915 species differ somewhat from each other. This study cannot distinguish whether modifications of the LH1 genes were induced or coordination and/or interaction modes of the metal cation with the binding sites of $\alpha\beta$ -polypeptides were altered during the biosynthetic replacement of Ca^{2+} with Sr^{2+} . There is

speculation that if the metal binding site of the Sr–LH1RC complex was biosynthetically altered to be optimal for Sr^{2+} , LH1RC forms reconstituted with Sr^{2+} should be the most stable, at least in the Sr^{2+} variant. However, the order of thermostability was identical for both the B888 and B915 species, and either Ca^{2+} or Ba^{2+} seems to be more suitable for enhancing the thermal stability of the core complex. In addition, if a modification of LH1 sequence was induced by this biosynthetic substitution, the time course of photosynthetic growth might involve a significant lag phase in the onset of growth on Sr^{2+} . However, this could not be confirmed in Figure 1. Accordingly, the properties of the metal binding site are presumed to be mostly retained between the Sr–LH1RC and Ca–LH1RC complexes despite some slight modifications that may result from the biosynthetic replacement of the metal cation. Nevertheless, we cannot exclude the possibility of a genetic modification in the LH1 complex, producing an LH1 protein sequence suitable for Sr^{2+} binding. The sequential analysis of LH1 $\alpha\beta$ -polypeptides from the Sr–LH1RC complex is in progress.

In this study, we report cultivation, purification, and characterization of the natural variant of LH1RC complexes from thermophilic *Tch. tepidum* in which Sr^{2+} was biosynthetically substituted for Ca^{2+} . This biosynthetic replacement is a valuable method for revealing roles of Ca^{2+} and structure–function relationships in this thermophilic organism without deterioration of the complexes and contamination with other metal cations during biochemical procedures. Further spectroscopic and thermodynamic analyses are currently in progress. These results will provide deeper insight into the Ca^{2+} binding site, which is necessary for understanding the roles of Ca^{2+} in the abnormal spectroscopic properties and enhanced thermal stability of *Tch. tepidum*.

■ ASSOCIATED CONTENT

Supporting Information. Absorption spectra of LH2 complexes from Ca- and Sr-*tepidum* cells (Figure S1), sodium dodecyl sulfate–polyacrylamide gel electrophoresis profiles of the purified LH1RC complex from Sr-*tepidum* cells (Figure S2), sucrose density gradient centrifugation analysis of Sr-*tepidum* cells (Figure S3), DSC profiles of LH1RCs from Ca-*tepidum* cells (Figure S4), and thermolysis of metal-substituted LH1RCs from Sr-*tepidum* cells (Figure S5). This material is available free of charge via the Internet at <http://pubs.acs.org>.

■ AUTHOR INFORMATION

Corresponding Author

*Telephone and fax: +81-78-803-5819. E-mail: ykimura@people.kobe-u.ac.jp.

Funding Sources

This research was supported by Grants-in-aid for Young Scientists (B) (20770102) (Y.K.) from the Ministry of Education, Culture, Sports, Science and Technology of Japan.

■ ABBREVIATIONS

BChl, bacteriochlorophyll; LH, light-harvesting; RC, reaction center; Ca-*tepidum*, wild-type *Tch. tepidum*; Sr-*tepidum*, *Tch. tepidum* in which Sr^{2+} is biosynthetically substituted for Ca^{2+} ; Sr- and Ca–LH1RC, LH1RC complex purified from Sr- and Ca-*tepidum*, respectively; DDPC, dodecylphosphocholine; OG, *n*-octyl β -D-glucopyranoside; EDTA, ethylenediaminetetraacetic acid; CD, circular

dichroism; MCD, magnetic circular dichroism; DSC, differential scanning calorimetry.

■ REFERENCES

- (1) Cogdell, R. J., Gall, A., and Kohler, J. (2006) The architecture and function of the light-harvesting apparatus of purple bacteria: From single molecules to *in vivo* membranes. *Q. Rev. Biophys.* 39, 227–324.
- (2) Deisenhofer, J., Epp, O., Miki, K., Huber, R., and Michel, H. (1985) Structure of the Protein Subunits in the Photosynthetic Reaction Center of *Rhodospseudomonas viridis* at 3 Å Resolution. *Nature* 318, 618–624.
- (3) Allen, J. P., Feher, G., Yeates, T. O., Rees, D. C., Deisenhofer, J., Michel, H., and Huber, R. (1986) Structural Homology of Reaction Centers from *Rhodospseudomonas sphaeroides* and *Rhodospseudomonas viridis* as Determined by X-ray-Diffraction. *Proc. Natl. Acad. Sci. U.S.A.* 83, 8589–8593.
- (4) Nogi, T., Fathir, I., Kobayashi, M., Nozawa, T., and Miki, K. (2000) Crystal structures of photosynthetic reaction center and high-potential iron-sulfur protein from *Thermochromatium tepidum*: Thermostability and electron transfer. *Proc. Natl. Acad. Sci. U.S.A.* 97, 13561–13566.
- (5) McDermott, G., Prince, S. M., Freer, A. A., Hawthornthwaite-Lawless, A. M., Papiz, M. Z., Cogdell, R. J., and Isaacs, N. W. (1995) Crystal-Structure of an Integral Membrane Light-Harvesting Complex from Photosynthetic Bacteria. *Nature* 374, 517–521.
- (6) Koepke, J., Hu, X. C., Muenke, C., Schulten, K., and Michel, H. (1996) The crystal structure of the light-harvesting complex II (B800–850) from *Rhodospirillum rubrum*. *Structure* 4, 581–597.
- (7) Roszak, A. W., Howard, T. D., Southall, J., Gardiner, A. T., Law, C. J., Isaacs, N. W., and Cogdell, R. J. (2003) Crystal structure of the RC-LH1 core complex from *Rhodospseudomonas palustris*. *Science* 302, 1969–1972.
- (8) Richter, M. F., Baier, J., Southall, J., Cogdell, R. J., Oellerich, S., and Kohler, J. (2007) Refinement of the X-ray structure of the RC LH1 core complex from *Rhodospseudomonas palustris* by single-molecule spectroscopy. *Proc. Natl. Acad. Sci. U.S.A.* 104, 20280–20284.
- (9) Karrasch, S., Bullough, P. A., and Ghosh, R. (1995) The 8.5-Ångström Projection Map of the Light-Harvesting Complex-I from *Rhodospirillum rubrum* Reveals a Ring Composed of 16 Subunits. *EMBO J.* 14, 631–638.
- (10) Fotiadis, D., Qian, P., Philippsen, A., Bullough, P. A., Engel, A., and Hunter, C. N. (2004) Structural analysis of the reaction center light-harvesting complex I photosynthetic core complex of *Rhodospirillum rubrum* using atomic force microscopy. *J. Biol. Chem.* 279, 20663–20668.
- (11) Scheuring, S., Francia, F., Busselez, J., Melandri, B. A., Rigaud, J. L., and Levy, D. (2004) Structural role of PufX in the dimerization of the photosynthetic core complex of *Rhodobacter sphaeroides*. *J. Biol. Chem.* 279, 3620–3626.
- (12) Qian, P., Hunter, C. N., and Bullough, P. A. (2005) The 8.5 Ångström projection structure of the core RC-LH1-PufX dimer of *Rhodobacter sphaeroides*. *J. Mol. Biol.* 349, 948–960.
- (13) Scheuring, S., Busselez, J., and Levy, D. (2005) Structure of the dimeric PufX-containing core complex of *Rhodobacter blasticus* by *in situ* atomic force microscopy. *J. Biol. Chem.* 280, 1426–1431.
- (14) Scheuring, S., Reiss-Husson, F., Engel, A., Rigaud, J. L., and Ranck, J. L. (2001) High-resolution AFM topographs of *Rubrivivax gelatinosus* light-harvesting complex LH2. *EMBO J.* 20, 3029–3035.
- (15) Scheuring, S., Seguin, J., Marco, S., Levy, D., Breyton, C., Robert, B., and Rigaud, J. L. (2003) AFM characterization of tilt and intrinsic flexibility of *Rhodobacter sphaeroides* light harvesting complex 2 (LH2). *J. Mol. Biol.* 325, 569–580.
- (16) Walz, T., Jamieson, S. J., Bowers, C. M., Bullough, P. A., and Hunter, C. N. (1998) Projection structures of three photosynthetic complexes from *Rhodobacter sphaeroides*: LH2 at 6 Ångström LH1 and RC-LH1 at 25 Ångström. *J. Mol. Biol.* 282, 833–845.
- (17) Scheuring, S., Rigaud, J. L., and Sturgis, J. N. (2004) Variable LH2 stoichiometry and core clustering in native membranes of *Rhodospirillum rubrum*. *EMBO J.* 23, 4127–4133.

- (18) Kereiche, S., Bourinet, L., Keegstra, W., Arteni, A. A., Verbavatz, J. M., Boekema, E. J., Robert, B., and Gall, A. (2008) The peripheral light-harvesting complexes from purple sulfur bacteria have different 'ring' sizes. *FEBS Lett.* 582, 3650–3656.
- (19) Angerhofer, A., Cogdell, R. J., and Hipkins, M. F. (1986) A Spectral Characterization of the Light-Harvesting Pigment-Protein Complexes from *Rhodospseudomonas acidophila*. *Biochim. Biophys. Acta* 848, 333–341.
- (20) Halloren, E., McDermott, G., Lindsay, J. G., Miller, C., Freer, A. A., Isaacs, N. W., and Cogdell, R. J. (1995) Studies on the Light-Harvesting Complexes from the Thermotolerant Purple Bacterium *Rhodospseudomonas cryptolactis*. *Photosynth. Res.* 44, 149–155.
- (21) Sturgis, J. N., Jirsakova, V., Reisschusson, F., Cogdell, R. J., and Robert, B. (1995) Structure and Properties of the Bacteriochlorophyll Binding Site in Peripheral Light-Harvesting Complexes of Purple Bacteria. *Biochemistry* 34, 517–523.
- (22) McLuskey, K., Prince, S. M., Cogdell, R. J., and Isaac, N. W. (2001) The crystallographic structure of the B800–820 LH3 light-harvesting complex from the purple bacteria *Rhodospseudomonas acidophila* strain 7050. *Biochemistry* 40, 8783–8789.
- (23) Evans, M. B., Hawthornthwaite, A. M., and Cogdell, R. J. (1990) Isolation and Characterization of the Different B800–850 Light-Harvesting Complexes from Low-Light and High-Light Grown Cells of *Rhodospseudomonas palustris*, Strain 2.1.6. *Biochim. Biophys. Acta* 1016, 71–76.
- (24) Tharia, H. A., Nightingale, T. D., Papiz, M. Z., and Lawless, A. M. (1999) Characterisation of hydrophobic peptides by RP-HPLC from different spectral forms of LH2 isolated from *Rps. palustris*. *Photosynth. Res.* 61, 157–167.
- (25) Hartigan, N., Tharia, H. A., Sweeney, F., Lawless, A. M., and Papiz, M. Z. (2002) The 7.5-Å electron density and spectroscopic properties of a novel low-light B800 LH2 from *Rhodospseudomonas palustris*. *Biophys. J.* 82, 963–977.
- (26) Cogdell, R. J., Gardiner, A. T., Roszak, A. W., Law, C. J., Southall, J., and Isaacs, N. W. (2004) Rings, ellipses and horseshoes: How purple bacteria harvest solar energy. *Photosynth. Res.* 81, 207–214.
- (27) Bahatyrova, S., Frese, R. N., van der Werf, K. O., Otto, C., Hunter, C. N., and Olsen, J. D. (2004) Flexibility and size heterogeneity of the LH1 light harvesting complex revealed by atomic force microscopy: Functional significance for bacterial photosynthesis. *J. Biol. Chem.* 279, 21327–21333.
- (28) McGlynn, P., Westerhuis, W. H. J., Jones, M. R., and Hunter, C. N. (1996) Consequences for the organization of reaction center-light harvesting antenna 1 (LH1) core complexes of *Rhodobacter sphaeroides* arising from deletion of amino acid residues from the C terminus of the LH1 α polypeptide. *J. Biol. Chem.* 271, 3285–3292.
- (29) Siebert, C. A., Qian, P., Fotiadis, D., Engel, A., Hunter, C. N., and Bullough, P. A. (2004) Molecular architecture of photosynthetic membranes in *Rhodobacter sphaeroides*: The role of PufX. *EMBO J.* 23, 690–700.
- (30) Wakao, N., Yokoi, N., Isoyama, N., Hiraishi, A., Shimada, K., Kobayashi, M., Kise, H., Iwaki, M., Itoh, S., Takaichi, S., and Sakurai, Y. (1996) Discovery of natural photosynthesis using Zn-containing bacteriochlorophyll in an aerobic bacterium *Acidiphilium rubrum*. *Plant Cell Physiol.* 37, 889–893.
- (31) Tuschak, C., Beatty, J. T., and Overmann, J. (2004) Photosynthesis genes and LH1 proteins of *Roseospiillum parvum* 930I, a purple non-sulfur bacterium with unusual spectral properties. *Photosynth. Res.* 81, 181–199.
- (32) Permentier, H. P., Neerken, S., Overmann, J., and Ames, J. (2001) A bacteriochlorophyll a antenna complex from purple bacteria absorbing at 963 nm. *Biochemistry* 40, 5573–5578.
- (33) Madigan, M. T. (1984) A Novel Photosynthetic Purple Bacterium Isolated from a Yellowstone Hot-Spring. *Science* 225, 313–315.
- (34) Madigan, M. T. (2003) Anoxygenic phototrophic bacteria from extreme environments. *Photosynth. Res.* 76, 157–171.
- (35) Kimura, Y., Hirano, Y., Yu, L. J., Suzuki, H., Kobayashi, M., and Wang, Z. Y. (2008) Calcium ions are involved in the unusual red shift of the light-harvesting 1 Q_y transition of the core complex in thermophilic purple sulfur bacterium *Thermochromatium tepidum*. *J. Biol. Chem.* 283, 13867–13873.
- (36) Kimura, Y., Yu, L. J., Hirano, Y., Suzuki, H., and Wang, Z. Y. (2009) Calcium ions are required for the enhanced thermal stability of the light-harvesting-reaction center core complex from thermophilic purple sulfur bacterium *Thermochromatium tepidum*. *J. Biol. Chem.* 284, 93–99.
- (37) Suzuki, H., Hirano, Y., Kimura, Y., Takaichi, S., Kobayashi, M., Miki, K., and Wang, Z. Y. (2007) Purification, characterization and crystallization of the core complex from thermophilic purple sulfur bacterium *Thermochromatium tepidum*. *Biochim. Biophys. Acta* 1767, 1057–1063.
- (38) Clayton, R. K., and Clayton, B. J. (1981) B850 Pigment-Protein Complex of *Rhodospseudomonas-sphaeroides*: Extinction Coefficients, Circular Dichroism, and the Reversible Binding of Bacteriochlorophyll. *Proc. Natl. Acad. Sci. U.S.A.* 78, 5583–5587.
- (39) Higuchi, M., Hirano, Y., Kimura, Y., Oh-oka, H., Miki, K., and Wang, Z. Y. (2009) Overexpression, characterization, and crystallization of the functional domain of cytochrome c(z) from *Chlorobium tepidum*. *Photosynth. Res.* 102, 77–84.
- (40) Georgakopoulou, S., van Grondelle, R., and van der Zwan, G. (2006) Investigation of the effects of different carotenoids on the absorption and CD signals of light harvesting 1 complexes. *J. Phys. Chem. B* 110, 3354–3361.
- (41) Kobayashi, M., Wang, Z. Y., Yoza, K., Umetsu, M., Konami, H., Mimuro, M., and Nozawa, T. (1996) Molecular structures and optical properties of aggregated forms of chlorophylls analyzed by means of magnetic circular dichroism. *Spectrochim. Acta, Part A* 52, 585–598.
- (42) Ma, F., Kimura, Y., Yu, L. J., Wang, P., Ai, X. C., Wang, Z. Y., and Zhang, J. P. (2009) Specific Ca²⁺-binding motif in the LH1 complex from photosynthetic bacterium *Thermochromatium tepidum* as revealed by optical spectroscopy and structural modeling. *FEBS J.* 276, 1739–1749.
- (43) Kuki, M., Naruse, M., Kakuno, T., and Koyama, Y. (1995) Resonance Raman Evidence for 15-Cis to All-Trans Photoisomerization of Spirilloxanthin Bound to a Reduced Form of the Reaction-Center of *Rhodospirillum rubrum* S1. *Photochem. Photobiol.* 62, 502–508.
- (44) Fiedor, L., Leupold, D., Teuchner, K., Voigt, B., Hunter, C. N., Scherz, A., and Scheer, H. (2001) Excitation trap approach to analyze size and pigment-pigment coupling: Reconstitution of LH1 antenna of *Rhodobacter sphaeroides* with Ni-substituted bacteriochlorophyll. *Biochemistry* 40, 3737–3747.
- (45) Hartwich, G., Fiedor, L., Simonin, I., Cmiel, E., Schafer, W., Noy, D., Scherz, A., and Scheer, H. (1998) Metal-substituted bacteriochlorophylls. I. Preparation and influence of metal and coordination on spectra. *J. Am. Chem. Soc.* 120, 3675–3683.
- (46) Jaschke, P. R., and Beatty, J. T. (2007) The photosystem of *Rhodobacter sphaeroides* assembles with zinc bacteriochlorophyll in a bchD (magnesium chelatase) mutant. *Biochemistry* 46, 12491–12500.
- (47) Boussac, A., Rappaport, F., Carrier, P., Verbavatz, J. M., Gobin, R., Kirilovsky, D., Rutherford, A. W., and Sugiura, M. (2004) Biosynthetic Ca²⁺/Sr²⁺ exchange in the photosystem II oxygen-evolving enzyme of *Thermosynechococcus elongatus*. *J. Biol. Chem.* 279, 22809–22819.
- (48) Blankenship, R. E. (1992) Origin and Early Evolution of Photosynthesis. *Photosynth. Res.* 33, 91–111.
- (49) Debus, R. J. (1992) The Manganese and Calcium-Ions of Photosynthetic Oxygen Evolution. *Biochim. Biophys. Acta* 1102, 269–352.
- (50) Aagaard, J., and Sistrom, W. R. (1972) Control of synthesis of reaction center bacteriochlorophyll in photosynthetic bacteria. *Photochem. Photobiol.* 15, 209–225.
- (51) Cogdell, R. J., Fyfe, P. K., Barrett, S. J., Prince, S. M., Freer, A. A., Isaacs, N. W., McGlynn, P., and Hunter, C. N. (1996) The purple bacterial photosynthetic unit. *Photosynth. Res.* 48, 55–63.
- (52) Solov'ev, A. A., and Erokhin, Y. E. (2008) Distribution of bacteriochlorophyll between the pigment-protein complexes of the sulfur photosynthetic bacterium *Allochromatium minutissimum* depending on light intensity at different temperatures. *Microbiology* 77, 534–540.
- (53) Nakagawa, K., Suzuki, S., Fujii, R., Gardiner, A. T., Cogdell, R. J., Nango, M., and Hashimoto, H. (2008) Electrostatic effect of surfactant

molecules on bacteriochlorophyll a and carotenoid binding sites in the LH1 complex isolated from *Rhodospirillum rubrum* S1 probed by Stark spectroscopy. *Photosynth. Res.* 95, 345–351.

(54) Yu, L. J., Kato, S., and Wang, Z. Y. (2010) Examination of the putative Ca^{2+} -binding site in the light-harvesting complex 1 of thermophilic purple sulfur bacterium *Thermochromatium tepidum*. *Photosynth. Res.* 106, 215–220.

(55) Kobayashi, M., Fujioka, Y., Mori, T., Terashima, M., Suzuki, H., Shimada, Y., Saito, T., Wang, Z. Y., and Nozawa, T. (2005) Reconstitution of photosynthetic reaction centers and core antenna-reaction center complexes in liposomes and their thermal stability. *Biosci., Biotechnol., Biochem.* 69, 1130–1136.

(56) Heda, G. D., and Madigan, M. T. (1988) Thermal-Properties and Oxygenase Activity of Ribulose-1,5-Bisphosphate Carboxylase from the Thermophilic Purple Bacterium, *Chromatium tepidum*. *FEMS Microbiol. Lett.* 51, 45–50.

(57) Heda, G. D., and Madigan, M. T. (1989) Purification and Characterization of the Thermostable Ribulose-1,5-Bisphosphate Carboxylase Oxygenase from the Thermophilic Purple Bacterium *Chromatium tepidum*. *Eur. J. Biochem.* 184, 313–319.